

# Manifold-Aware Deep Clustering: Maximizing Angles between Embedding Vectors Based on Regular Simplex

Keitaro Tanaka<sup>†\*</sup>, Ryosuke Sawata<sup>‡</sup>, Shusuke Takahashi<sup>‡</sup>

<sup>†</sup>Waseda University, Japan, <sup>‡</sup>Sony Corporation, Japan

phys.keitaro1227@ruri.waseda.jp, {Ryosuke.Sawata, Shusuke.Takahashi}@sony.com

## Abstract

This paper presents a new deep clustering (DC) method called manifold-aware DC (M-DC) that can enhance hyperspace utilization more effectively than the original DC. The original DC has a limitation in that a pair of two speakers has to be embedded having an orthogonal relationship due to its use of the one-hot vector-based loss function, while our method derives a unique loss function aimed at maximizing the target angle in the hyperspace based on the nature of a regular simplex. Our proposed loss imposes a higher penalty than the original DC when the speaker is assigned incorrectly. The change from DC to M-DC can be easily achieved by rewriting just one term in the loss function of DC, without any other modifications to the network architecture or model parameters. As such, our method has high practicability because it does not affect the original inference part. The experimental results show that the proposed method improves the performances of the original DC and its expansion method.

**Index Terms:** Deep clustering, Chimera network, speech separation, hypersphere manifold embedding.

## 1. Introduction

Monaural speech separation is a fundamental task for automatic speech recognition (ASR) [1]. Before the widespread use of deep learning methods, most speech separation approaches focused on scenarios with multiple microphones [2, 3], and a monaural scenario remained a challenging task. Since deep neural networks (DNNs) have appeared, a straightforward approach for this task has been to train a DNN in a supervised manner using pairs of mixture sound and separated sounds [4]. In these methods, one separation is generally performed per short duration since such processing is convenient in terms of the calculation cost, simplicity to exploit, later application (e.g., ASR) and so on. However, this causes a permutation problem that makes considering the consistency of output tracks difficult because each DNN-based separation is conducted per short duration independently. For example, even if a temporary separation is successful, the speaker of the current 1st track is not always the same as the speaker of the previous 1st track or the next 1st track, which may be swapped with the speaker of 2nd track. There are two main approaches to avoiding this problem, and several DNN-based source separation methods using these approaches have been studied [5–9].

The first approach involves permutation invariant training (PIT) [5–7]. This method considers all possible correspondences between the outputs of a DNN and the speakers included

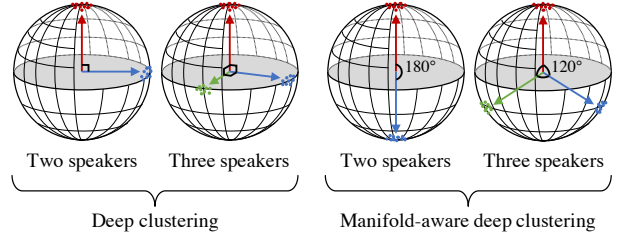


Figure 1: *The proposed method maximizes the target angle between two embeddings from different speakers. The target angle differs depending on the number of speakers.*

in a mixture sound. The actual optimization of the network is then conducted only for the best permutation among them. By considering all possible correspondences, PIT allows a DNN to be trained directly. Furthermore, PIT works with any DNN output, including short-time Fourier transform (STFT) magnitudes [5–7] and waveforms [10–13]. Methods with waveform outputs have been particularly widely used because of their excellent quality (e.g., Conv-TasNet [10], Dual-path RNN [11], and Nachmani *et al.* [12]) and are currently the leading solutions for speaker-independent monaural speech separation. Most recently, Zeghidour *et al.* have proposed Wavesplit [13], which achieves a state-of-the-art performance.

The second approach is to use deep clustering (DC) [8, 9], which estimates a high-dimensional embedding for each time-frequency (TF) bin of an input spectrogram such that two embeddings are close to or far from each other depending on whether they belong to the same speaker or not. TF bins are grouped in accordance with speakers by means of a clustering technique (e.g., *k*-means [14]) in the embedding space at a later stage. Since the clustering technique is a non-supervised method and can group arbitrary embeddings by speakers regardless of the time duration, DC can select a consistent track with the same speaker. In this way, DC solves the permutation problem by avoiding the need for direct mask estimation. Inspired by this approach, many improved versions of DC have been proposed [3]. For example, the deep attractor network [15–17] estimates not only embeddings but also the centroids of embeddings, and the Chimera network [18, 19] estimates both binary masks and ratio masks. In addition, DC has been used in music information retrieval tasks, such as the Cerberus network [20] and instrument-independent music transcription [21], indicating its potential for various applications.

Despite the advances mentioned above, the nature of the embedding space in DC has not been studied sufficiently. In general, the loss function of DC defines the *correct* target distances between all pairs of embeddings of TF bins by using one-hot vectors. In terms of the manifold perspective, the embeddings belonging to different speakers are forced to locate in an orthogonal way on a hyperspherical space, since the representation of one-hot vectors corresponds to 90 degrees by handling

\*Work done during an internship at Sony. Keitaro Tanaka wishes to express the deepest gratitude to Prof. Shigeo Morishima at Waseda Research Institute for Science and Engineering, Tokyo, Japan. Keitaro Tanaka was fully supported by JST Mirai Program No. JPMJMI19B2, and JSPS KAKENHI Nos. 19H01129 and 19H04137 in the publication of this paper and participation in the conference.

their vectors using a cosine function. As an example, the vectors of DC are illustrated on the left side of Fig. 1. This orthogonal constraint causes inefficient use of the embedding space with respect to each input mixture, resulting in performance deterioration of DC.

In order to solve this problem, we propose a manifold-aware DC (M-DC) that renews the definition of target embedding distances. To utilize the whole embedding space for each mixture, we maximize the target angle based on the number of speakers, as shown in Fig. 1. Specifically, we rewrite the original DC loss function to modify target cosine distances on a manifold hypersphere by considering the nature of a regular simplex [22–24]. In our method, this newly derived cosine distance enables M-DC to impose a smaller or greater penalty to embeddings depending on whether they are easy or difficult to separate from already embedded speakers. This effect leads to clustering-friendly embedding at the later stage. Therefore, M-DC can discriminate the speakers more effectively than the original DC.

The main contribution of this paper is the operation of DC with a unique loss function for efficient learning based on full utilization of the hyperspherical embedding space with respect to each input mixture. The change from DC to M-DC can be achieved by rewriting just one term in the loss function of DC, without any other modifications to the network architecture or model parameters.

## 2. Proposed Method

Our goal with M-DC is to train the DC network while enhancing the utilization of its hyperspherical embedding space. Specifically, M-DC maximizes each of the angles between two speakers, which are shaped in the embedding space.

### 2.1. Brief Review of Deep Clustering

Since our method is partly based on the original DC, we first review DC here briefly.

DC separates the input mixture speech in the STFT domain by assigning a  $D$ -dimensional normalized embedding to each TF bin using a DNN. The network is trained such that embeddings belonging to the same speaker are close to each other, and those belonging to different speakers are far from each other. Let  $\mathbf{V} \in \mathbb{R}^{TF \times D}$  and  $\mathbf{Y} \in \{0, 1\}^{TF \times N}$  be the normalized embeddings estimated by a DNN and the dominant speaker indicators ( $(\mathbf{Y})_{in} = 1$  if speaker  $n$  is dominant in the  $i$ th TF bin  $(t, f)$ , and  $(\mathbf{Y})_{in} = 0$  otherwise), where  $T$ ,  $F$ , and  $N$  respectively represent the numbers of time frames, frequency bins, and speakers included in the mixture spectrogram. DC brings the cosine distances between all embedding pairs close to the *correct* target ones by minimizing the loss function  $\mathcal{L}_{DC}$ , calculated as

$$\mathcal{L}_{DC} = \|\mathbf{V}\mathbf{V}^T - \mathbf{Y}\mathbf{Y}^T\|_F^2 \quad (1)$$

$$= \|\mathbf{V}^T \mathbf{V}\|_F^2 + \|\mathbf{Y}^T \mathbf{Y}\|_F^2 - 2\|\mathbf{V}^T \mathbf{Y}\|_F^2, \quad (2)$$

where  $\|\cdot\|_F$  denotes the Frobenius norm of a matrix.  $\mathbf{V}\mathbf{V}^T \in \mathbb{R}^{TF \times TF}$  shows the cosine distances between all embedding pairs, while  $\mathbf{Y}\mathbf{Y}^T \in \mathbb{R}^{TF \times TF}$  shows the *correct* target ones. Note that  $(\mathbf{Y}\mathbf{Y}^T)_{i_1 i_2} = 1$  if the  $i_1$ th and  $i_2$ th TF bins belong to the same speaker, and  $= 0$  otherwise. Since a DC network well-trained by the above  $\mathcal{L}_{DC}$  enables the embeddings to get close to others obtained from the same speakers, assigning the TF bins to the correct speakers, *i.e.*, clustering, becomes feasible.

### 2.2. Manifold-Aware Deep Clustering

In general, to utilize the hyperspace effectively with respect to each input mixture, it is desirable to divide the whole hypersphere into  $N$ , *i.e.*, the total number of speakers. Specifically, the hypersphere is divided by  $N$  speakers equally so that each angle is equal to  $\arccos\{-1/(N-1)\}$ . For example, each optimal angle is 180 degrees ( $= \arccos\{-1/(2-1)\}$ ) if there are two speakers, and then its relationship between the embedded points is equal to a straight line, which is a 1-dimensional regular simplex [22, 24]. When there are three speakers, each optimal angle is 120 degrees ( $= \arccos\{-1/(3-1)\}$ ), and then its relationship among embedded points is equal to an equilateral triangle, which is a 2-dimensional regular simplex. Similarly, such a relationship among four embedded speakers makes a regular tetrahedron, which is a 3-dimensional regular simplex. On the basis of this discussion, we inductively estimate that the embedded  $N$  speakers make an  $(N-1)$ -dimensional regular simplex.

Therefore, to improve the hyperspace utilization of the original DC, the key thing to consider is the characteristics of the regular simplex.

#### 2.2.1. Introduction of Regular Simplex

In order to enhance the utilization of a  $D$ -dimensional hyperspace, our goal is to determine the best  $N$  points on a hypersphere (*i.e.*, a  $(D-1)$ -dimensional hypersphere) so that they are distributed as far away from each other as possible. Note that the number of dimensions  $D$  is appropriately large ( $D \geq N-1$ ) for the given  $N (\geq 2)$ . Under the aforementioned condition, we consider that the vertices of an  $(N-1)$ -dimensional regular simplex are equivalent to the best  $N$  positions, as described above.

First, we show that the positional relationship we look for needs to be that of the vertices of a regular simplex. To ensure the symmetry among all points, they have to be located point-symmetrically with respect to the center of the hyperball. Therefore, the  $D$ -dimensional Euclidean distances between all pairs of the points are equal to each other. In addition, for  $R \leq N-1$ , none of the  $R+1$  points can be contained in an  $(R-1)$ -dimensional hyperplane at the same time. This situation precisely meets the definition of a regular simplex.

Next, we conversely show that the positional relationship of the vertices of a regular simplex can meet the relationship we look for. An  $(N-1)$ -dimensional regular simplex can be embedded in a  $D$ -dimensional hyperball with a  $(D-1)$ -dimensional hypersphere under the condition of  $D \geq N-1$ . When  $D > N-1$ , the dimensions of  $D-N+1$  create extra dimensions during the embedding. Due to the nature of the regular simplex, the vertices are necessarily point-symmetric with respect to the center and are located farthest away from each other. Therefore, the two relationships are indeed equivalent.

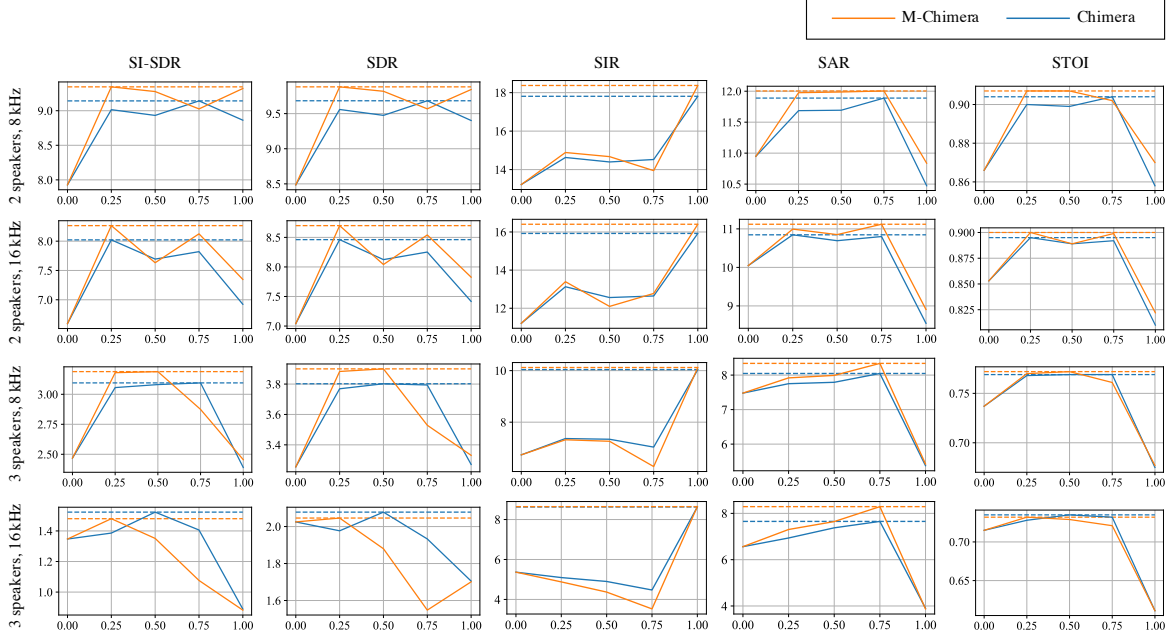
#### 2.2.2. New Definition of Target Cosine Distance

Motivated by the above discussion, we embed the mixed speakers as  $N$  points in such a manner that the positional relationship meets the vertices of an  $(N-1)$ -dimensional regular simplex. We can embed an  $(N-1)$ -dimensional regular simplex in a normalized hyperball by considering  $N$  points  $\{\mathbf{x}_n\}_{n=1}^N$ , where their coordinates from the centroid are represented as

$$\left( \underbrace{\dots, \frac{-1}{N} \sqrt{\frac{N}{N-1}}, \frac{N-1}{N} \sqrt{\frac{N}{N-1}}}_{n-1}, \underbrace{\frac{-1}{N} \sqrt{\frac{N}{N-1}}, \dots}_{N-n} \right). \quad (3)$$

Table 1: Separation results of DC and M-DC. Scores written in bold are the higher one(s).

Configuration	SI-SDR		SDR		SIR		SAR		STOI	
	DC	M-DC	DC	M-DC	DC	M-DC	DC	M-DC	DC	M-DC
2 speakers, 8 kHz	8.863	<b>9.321</b>	9.402	<b>9.843</b>	17.810	<b>18.372</b>	10.473	<b>10.837</b>	0.858	<b>0.870</b>
2 speakers, 16 kHz	6.923	<b>7.347</b>	7.417	<b>7.827</b>	15.923	<b>16.405</b>	8.548	<b>8.907</b>	0.810	<b>0.822</b>
3 speakers, 8 kHz	2.390	<b>2.455</b>	3.271	<b>3.331</b>	10.041	<b>10.121</b>	5.376	<b>5.423</b>	0.675	<b>0.677</b>
3 speakers, 16 kHz	<b>0.889</b>	0.882	<b>1.705</b>	1.701	8.629	<b>8.645</b>	<b>3.900</b>	3.874	<b>0.611</b>	<b>0.611</b>


 Figure 2: Separation results of the Chimera network with DC (Chimera) and with M-DC (M-Chimera). Dashed lines show the best scores of each method under the configuration. The horizontal axis represents  $\alpha$ . M-Chimera is equivalent to Chimera when  $\alpha=0$ .

Then, the inner products of pairs of these vectors are calculated as

$$\langle \mathbf{x}_{n_1}, \mathbf{x}_{n_2} \rangle = \begin{cases} 1 & (n_1 = n_2) \\ -\frac{1}{N-1} & (n_1 \neq n_2), \end{cases} \quad (4)$$

where  $\langle \cdot, \cdot \rangle$  denotes the inner product of two vectors. Equation (4) ensures that the regular simplex just fits in a normalized hyperball (*i.e.*, the vertices touch a normalized hypersphere), while Eq. (5) gives the new target cosine distance. Consequently, maximization of the angle corresponding to this cosine distance, *i.e.*,  $\arccos\{-1/(N-1)\}$ , becomes feasible.

Equations (3), (4), and (5) also show that M-DC gets closer to the original DC when  $N$  increases. M-DC theoretically matches the original DC in a situation with an infinite number of speakers  $N$ , as follows:

$$\text{Eq. (3)} \xrightarrow{N \rightarrow \infty} (\underbrace{\dots, 0}_{n-1}, \underbrace{1, 0, \dots}_{N-n}), \quad (6)$$

$$\text{Eq. (4)} \xrightarrow{N \rightarrow \infty} 1 (= \cos(0)), \quad (7)$$

$$\text{Eq. (5)} \xrightarrow{N \rightarrow \infty} 0 (= \cos(90)). \quad (8)$$

As shown in Eqs. (7) and (8), each of the angles among all embedded points is 90 degrees, *i.e.*, orthogonal, when assuming the total number of speakers is infinity, and this is equal to the original DC's loss due to using one-hot vector, like Eq. (6). Hence, M-DC is equal to the original DC when the total number of speakers  $N$  is infinity. In other words, M-DC is theoretically

equivalent or superior to the original DC since  $N$  is actually a finite value.

### 2.2.3. Manifold-Aware Deep Clustering Training

M-DC not only maximizes the angle between two embeddings belonging to different speakers but also allows the use of previously untouched sides of the hypersphere due to its overall symmetry. This theoretically enables us to train a DNN having maximum spatial efficiency for each mixture. Furthermore, the only difference between DC and M-DC in the actual training is exactly one term of  $\mathcal{L}_{\text{DC}}$  (*i.e.*,  $\mathbf{Y}$ , not  $\mathbf{Y}\mathbf{Y}^\top$ ). Since it is difficult to calculate  $\mathcal{L}_{\text{DC}}$  directly defined in Eq. (1) because of its high computational cost,  $\mathcal{L}_{\text{DC}}$  is actually calculated with its expanded form (Eq. (2)). On the basis of Eqs. (3)–(5), we can define the single term  $\mathbf{Y}$  for M-DC as follows:

$$\mathbf{Y} = (\underbrace{\dots, \mathbf{y}_i, \dots}_{TF})^\top, \quad (9)$$

where  $\mathbf{y}_i = \mathbf{x}_n^\top$  if speaker  $n$  is dominant in the  $i$ th TF bin.

In summary, substituting our new  $\mathbf{Y}$  defined in Eq. (9) for Eq. (2) means we can easily achieve M-DC. Hence, changing M-DC from the original DC becomes feasible without any other modifications to the network architecture or model parameters.

## 3. Evaluation

In this section, we evaluate the proposed method by replacing the original DC in two well-known methods with our M-DC: i) the original DC itself and ii) the DC-based Chimera network.

### 3.1. Data

In our evaluation, we used the WSJ0-2mix and WSJ0-3mix datasets [8], which contain 30 hours of two- and three-speaker speech mixtures for training and ten hours for validation. The evaluation sets contain five hours of two- and three-speaker speech mixtures, where the speakers are not shared between the training or the validation sets and the evaluation sets. All sounds were resampled to 8 kHz and 16 kHz. We used STFT with the square root of a Hann window of 256 samples and a shifting interval of 64 samples, *i.e.*, 75% overlapped, to obtain the spectrogram.

### 3.2. Model Configurations

The DC network had four bi-directional long short-term memory (BLSTM) layers followed by one feedforward layer. Each BLSTM layer had 600 hidden cells, and the feedforward layer corresponded to the embedding dimensions, which we set to  $D = 40$ . The Chimera network had a similar architecture except that the feedforward layer was split into two. One was the same as the DC network (DC head), while the other corresponded to the number of speakers (MI head) for direct mask inference. We used rmsprop optimization [25] with an initial learning rate of  $10^{-4}$ . We dropped the learning rate by 0.5 if the validation loss did not decrease after five epochs. We stopped the training if the validation loss did not decrease after thirty epochs and then selected the network on the basis of the validation loss. The batch size was 32. Our implementation used Asteroid [26], the PyTorch-based audio source separation toolkit.

### 3.3. Evaluation Criteria

We evaluated M-DC in terms of five criteria: scale-invariant signal-to-distortion ratio (SI-SDR) in dB [27], signal-to-distortion ratio (SDR) in dB [28], signal-to-interference ratio (SIR) in dB [28], signal-to-artifacts ratio (SAR) in dB [28], and short-time objective intelligibility (STOI) ranging from 0 to 1 [29]. We calculated the averages of the above criteria for each speaker. The performance on DC was evaluated with a different number of speakers (two or three) and different sampling rates (8 kHz or 16 kHz). Clustering at a later stage was conducted by  $k$ -means. The performance on the Chimera network was additionally evaluated for different hyperparameter values  $\alpha \in \{0, 0.25, 0.5, 0.75, 1.0\}$ , which controls the weight between the two heads (only MI head or DC head was used when  $\alpha = 0$  or  $\alpha = 1$ ). The sound separation was conducted by the MI head (*i.e.*, by estimated ratio masks) except in the case of  $\alpha = 1$  (*i.e.*, by estimated binary masks).

### 3.4. Experimental Results

The experimental results are shown in Table 1 and Fig. 2. First, Table 1 shows that our M-DC outperformed the original DC in almost all cases. In particular, our performances regarding two speakers were significantly superior to those of DC. While we found that the degrees of improvement in the case of three speakers were less than those of two speakers, they were comparable to the original DC's ones. This is because, as we explained in Sec. 2.2.2 (see Eqs. (6)–(8)), the performance of M-DC got close to that of the original DC by increasing the number of speakers  $N$ , *i.e.*, from 2 to 3, in these experiments. Hence, our assumption regarding the relationship between the original DC and our M-DC described in Sec. 2.2.2 is correct.

Next, we focus on the results of the DC-based expansion method, *i.e.*, the Chimera network. From Fig. 2, we can see that almost all our best scores were superior to those of the original Chimera network (as indicated by the dashed line). In addition,

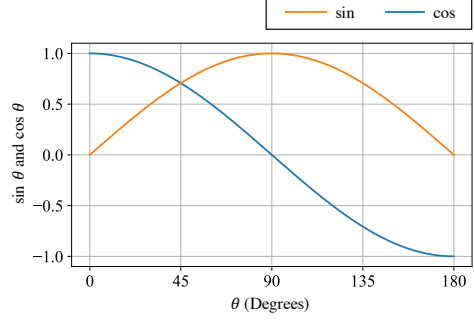


Figure 3: The sine represents the absolute value of the gradient of the cosine, which reaches its maximum at 90 degrees.

we confirmed a tendency that was similar to the previous results, *i.e.*, M-DC getting close to DC by increasing the number of speakers.

Here, we focus on the difference of the optimal  $\alpha$  between DC and M-DC loss. Since both methods learn based on the cosine distance, we presume that the training depends on the value of the cosine's gradient. Specifically, a large penalty is imposed to the angle when the absolute value of the gradient of the cosine (*i.e.*, the value of the sine) is large, as shown in Fig. 3. This suggests that the orthogonal position, *i.e.*,  $\sin(90)$ , has the highest influence on the training due to having the highest value in Fig. 3. As shown in Fig. 1, in DC, the orthogonal position is equal to the different speaker. On the other hand, in M-DC, the orthogonal position is equal to the ambiguous speaker (not the different one) since our M-DC locates a different speaker having more than 90 degrees, *e.g.*, 180 and 120 degrees when the number of speakers  $N$  is 2 and 3. In other words, the orthogonal position in our M-DC means the ambiguous speaker, since the 90 degrees is under both 180 and 120 degrees, and thus our M-DC was trained by focusing more on the difficult (= ambiguous) cases than the original DC. These results demonstrate that our M-DC can deliver a more robust and effective performance than the original DC. This effect also resulted in the difference of the best  $\alpha$  in the Chimera network.

## 4. Conclusion

In this paper, we presented M-DC, which improves the original DC by using a unique loss function for efficient learning. We fully utilized the hyperspherical embedding space by newly defining a target embedding distance by means of a loss function depending on the number of speakers. The change from DC to M-DC was easily achieved by modifying just one term of the loss function, and thus has no effect on the original DC's inference part. Furthermore, since not only the original DC but also the DC-based expansion methods can be improved by introducing our M-DC, as demonstrated in our experiments, we argue that M-DC has high practicability for many existing DC-based methods.

In future work, we will evaluate the performance improvement based on the clustering accuracy itself. We also plan to conduct additional evaluations on cases of more than three speakers and in other DC-based techniques. In this work, we let M-DC create extra dimensions, and although we think these dimensions enrich a DNN's expression ability, there is a room for making the model more compact by means of dimensional reduction. Another interesting direction would be to combine our method with other clustering techniques [30], which would result in an even better performance. We believe the findings of our work will contribute to the further development of DC.

## 5. References

- [1] Y. Dong and L. Deng, *Automatic Speech Recognition: A Deep Learning Approach*. Springer, 2014.
- [2] K. Farrell, R. J. Mammone, and J. L. Flanagan, “Beamforming microphone arrays for speech enhancement,” in *IEEE International Conference on Acoustics, Speech and Signal Processing (ICASSP)*, 1992, pp. 285–288.
- [3] R. Aihara, G. Wichern, and J. L. Roux, “Deep clustering-based single-channel speech separation and recent advances,” *Acoustical Science and Technology*, vol. 41, no. 2, pp. 465–471, 2020.
- [4] J. R. Hershey, S. J. Rennie, P. A. Olsen, and T. T. Kristjansson, “Super-human multi-talker speech recognition: A graphical modeling approach,” *Computer Speech & Language*, vol. 24, pp. 45–66, 2010.
- [5] D. Yu, M. Kolbæk, Z.-H. Tan, and J. Jensen, “Permutation invariant training of deep models for speaker-independent multi-talker speech separation,” in *IEEE International Conference on Acoustics, Speech and Signal Processing (ICASSP)*, 2017, pp. 241–245.
- [6] M. Kolbæk, D. Yu, Z.-H. Tan, and J. Jensen, “Multitalker speech separation with utterance-level permutation invariant training of deep recurrent neural networks,” *IEEE/ACM Transactions on Audio, Speech, and Language Processing (TASLP)*, vol. 25, no. 10, pp. 1901–1913, 2017.
- [7] C. Xu, W. Rao, X. Xiao, E. S. Chng, and H. Li, “Single channel speech separation with constrained utterance level permutation invariant training using grid LSTM,” in *IEEE International Conference on Acoustics, Speech and Signal Processing (ICASSP)*, 2018, pp. 6–10.
- [8] J. R. Hershey, Z. Chen, J. L. Roux, and S. Watanabe, “Deep clustering: Discriminative embeddings for segmentation and separation,” in *IEEE International Conference on Acoustics, Speech and Signal Processing (ICASSP)*, 2016, pp. 31–35.
- [9] Y. Isik, J. L. Roux, Z. Chen, S. Watanabe, and J. R. Hershey, “Single-channel multi-speaker separation using deep clustering,” in *Annual Conference of the International Speech Communication Association (Interspeech)*, 2016, pp. 545–549.
- [10] Y. Luo and N. Mesgarani, “Conv-TasNet: Surpassing ideal time–frequency magnitude masking for speech separation,” *IEEE/ACM Transactions on Audio, Speech, and Language Processing (TASLP)*, vol. 27, no. 8, pp. 1256–1266, 2019.
- [11] Y. Luo, Z. Chen, and T. Yoshioka, “Dual-Path RNN: Efficient long sequence modeling for time-domain single-channel speech separation,” in *IEEE International Conference on Acoustics, Speech and Signal Processing (ICASSP)*, 2020, pp. 46–50.
- [12] E. Nachmani, Y. Adi, and L. Wolf, “Voice separation with an unknown number of multiple speakers,” in *International Conference on Machine Learning (ICML)*, 2020, pp. 7164–7175.
- [13] N. Zeghidour and D. Grangier, “Wavesplit: End-to-end speech separation by speaker clustering,” in *arXiv preprint arXiv:2002.08933*, 2020.
- [14] S. P. Lloyd, “Least squares quantization in PCM,” *IEEE Transactions on Information Theory*, vol. 28, no. 2, pp. 129–137, 1982.
- [15] Z. Chen, Y. Luo, and N. Mesgarani, “Deep attractor network for single-microphone speaker separation,” in *IEEE International Conference on Acoustics, Speech and Signal Processing (ICASSP)*, 2017, pp. 246–250.
- [16] Y. Luo, Z. Chen, and N. Mesgarani, “Speaker-independent speech separation with deep attractor network,” *IEEE/ACM Transactions on Audio, Speech, and Language Processing (TASLP)*, vol. 26, no. 4, pp. 787–796, 2018.
- [17] C. Cadoux, S. Uhlich, M. Ferras, and Y. Mitsufuji, “Closing the training/inference gap for deep attractor networks,” in *arXiv preprint arXiv:1911.02091*, 2019.
- [18] Y. Luo, Z. Chen, J. R. Hershey, J. L. Roux, and N. Mesgarani, “Deep clustering and conventional networks for music separation: Stronger together,” in *IEEE International Conference on Acoustics, Speech and Signal Processing (ICASSP)*, 2017, pp. 61–65.
- [19] Z.-Q. Wang, J. L. Roux, and J. R. Hershey, “Alternative objective functions for deep clustering,” in *IEEE International Conference on Acoustics, Speech and Signal Processing (ICASSP)*, 2018, pp. 686–690.
- [20] E. Manilow, P. Seetharaman, and B. Pardo, “Simultaneous separation and transcription of mixtures with multiple polyphonic and percussive instruments,” in *IEEE International Conference on Acoustics, Speech and Signal Processing (ICASSP)*, 2020, pp. 771–775.
- [21] K. Tanaka, T. Nakatsuka, R. Nishikimi, K. Yoshii, and S. Morishima, “Multi-instrument music transcription based on deep spherical clustering of spectrograms and pitchgrams,” in *International Society for Music Information Retrieval Conference (ISMIR)*, 2020, pp. 327–334.
- [22] H. S. M. Coxeter, *Regular Polytopes*. Dover Publications, 1973.
- [23] W. Rudin, *Principles of mathematical analysis*. New York: McGraw-Hill, 1976.
- [24] E. L. Elte, *The semiregular polytopes of the hyperspaces*. Michigan: University of Michigan Library, 2005.
- [25] T. Tieleman and G. Hinton, “Lecture 6.5-rmsprop, coursera: Neural networks for machine learning,” *University of Toronto, Technical Report*, 2012.
- [26] M. Pariente, S. Cornell, J. Cosentino, S. Sivasankaran, E. Tzinis, J. Heitkaemper, M. Olvera, F.-R. Stöter, M. Hu, J. M. Martín-Doñas, D. Ditter, A. Frank, A. Deleforge, and E. Vincent, “Asteroïd: the PyTorch-based audio source separation toolkit for researchers,” in *Annual Conference of the International Speech Communication Association (Interspeech)*, 2020, pp. 2637–2641.
- [27] J. L. Roux, S. Wisdom, H. Erdogan, and J. R. Hershey, “SDR – half-baked or well done?” in *IEEE International Conference on Acoustics, Speech and Signal Processing (ICASSP)*, 2019, pp. 626–630.
- [28] E. Vincent, R. Gribonval, and C. Févotte, “Performance measurement in blind audio source separation,” *IEEE/ACM Transactions on Audio, Speech, and Language Processing (TASLP)*, vol. 14, no. 4, pp. 1462–1469, 2006.
- [29] C. H. Taal, R. C. Hendriks, R. Heusdens, and J. Jensen, “A short-time objective intelligibility measure for time-frequency weighted noisy speech,” in *IEEE International Conference on Acoustics, Speech and Signal Processing (ICASSP)*, 2010, pp. 4214–4217.
- [30] Y. Luo and N. Mesgarani, “Augmented time-frequency mask estimation in cluster-based source separation algorithms,” in *IEEE International Conference on Acoustics, Speech and Signal Processing (ICASSP)*, 2019, pp. 710–714.